

Large orbital eccentricities and close encounters at the 2:1 resonance of a dynamical system modelling asteroidal motion

H. Varvoglis

Department of Physics, Section of Astrophysics, Astronomy and Mechanics, University of Thessaloniki, GR-540 06 Thessaloniki, Greece

Received May 18, 1992; accepted February 11, 1993

Abstract. In a recent work (Varvoglis 1991) we proposed the use of a model dynamical system as a fast and effective method to study the motion of asteroids in the main asteroidal belt. This dynamical system is, essentially, a modified planar elliptical restricted three-body problem, in which the variation of Jupiter's eccentricity, caused by the perturbation of Saturn, is taken explicitly into account. Here we show that, near the 2:1 resonance, the (osculating) eccentricity, e , of the trajectories of this dynamical system may attain high values ($e \geq 0.6$) and that a fictitious asteroid, following such a "high- e " trajectory, may undergo a close encounter with Jupiter and be subsequently removed from the 2:1 resonance region.

Key words: celestial mechanics, stellar dynamics – minor planets

1. Introduction

The presently most favoured model for the creation of the Kirkwood gaps in the asteroidal belt is based on the work of Wisdom (1982, 1983, 1987) on the 3:1 resonance of the planar elliptical restricted three body problem (ERTBP). Wisdom showed that, in the case of this resonance, the osculating eccentricity, e , of a fictitious asteroid's trajectory undergoes chaotic variations and that, during this phenomenon, e may become large enough, so as to transform this asteroid to a Mars crosser. Such an asteroid may then be removed from the distribution through a close encounter with Mars. Subsequent studies (e.g. see Lemaître & Henrard 1990) showed that the above model cannot explain the gap at the 2:1 resonance, since in this case the eccentricity of the asteroids' trajectories varies within relatively low values up to the longest time interval of numerical integrations. We note for later reference that, in the 2:1 resonance region, an asteroid becomes Mars crosser for $e > e_{\text{crit}}^I = 0.52$ and Jupiter crosser for $e > e_{\text{crit}}^{II} = 0.58$.

Wisdom (1987) and Yoshikawa (1989, 1991) have found that the integration of the full, three-dimensional, four-body problem (Sun–Jupiter–Saturn–asteroid) showed an increase of e above e_{crit}^I , mainly for trajectories initially in the unstable configuration (see Sect. 2) and at the boundaries of the resonant gap. However, it was not clear which of the added degrees of freedom was the dominant one in producing this effect (e.g. see Wisdom 1987). In a recent work (Varvoglis 1991, hereafter referred to as Paper I) we proposed the use of a model dynamical system as a means to describe, qualitatively, the motion of asteroids in the asteroidal belt faster and, therefore, more efficiently than through the integration of the four-body problem. In this dynamical system the variation of the eccentricity, e_j , of Jupiter's orbit, which originates in the perturbations of Saturn, is introduced explicitly by hand in the equations of motion of the ERTBP. In Paper I the form of the variation was taken to be sinusoidal, while, in order to further accelerate the calculations, its period, T_{ej} , was generally taken smaller than the actual one ($\approx 10^3 T_J$, where by T_J we denote the period of revolution of Jupiter around the Sun), a technique well known in plasma physics (e.g. see Hockney & Eastwood 1981). The appearance of eccentricities larger than e_{crit}^I in trajectories of this model dynamical system near the 2:1 resonance turned out to be not uncommon, at least for trajectories starting at the unstable configuration with $T_{ej}/T_J \approx 10$ studied extensively in Paper I. In the same paper it was argued that the results obtained for $T_{ej}/T_J < 10^3$ may be extrapolated to the actual period of the phenomenon, since in numerical studies with successively larger values of T_{ej}/T_J the qualitative behaviour of the trajectories remains essentially the same.

In this work we show that the trajectories of fictitious asteroids in the 2:1 resonance of our model dynamical system described above, starting either at the stable or the unstable configuration, not only attain eccentricities exceeding e_{crit}^{II} but may even undergo a close encounter with Jupiter. In this context we present a typical case where, after a close encounter with Jupiter, the asteroid is removed

from the 2:1 resonance and, in the absence of perturbations from other planets (which are not included in our model), it follows a trajectory lying outside the orbit of Jupiter.

2. Description of the model and results

The dynamical system we are using to model the motion of an asteroid is a modification of the ERTBP, in which e_j is taken to vary sinusoidally with time between two extreme values, $e_{j\min}$ and $e_{j\max}$, starting at $e_{j0} = (e_{j\min} + e_{j\max})/2$ (for details see Paper I). The co-ordinate system used is a heliocentric rotating pulsating one, in which the units of time, length and mass are the usual ones, namely $T_J/2\pi$, α_J and $M_S + M_J$ respectively, where by α_J we denote the semi-major axis of Jupiter's orbit and by M_J and M_S the masses

of Jupiter and the Sun. The calculated trajectories of this dynamical system are organised in "families". The initial conditions of the trajectories of each family are computed, to facilitate comparison with older results, from the corresponding trajectory of the circular restricted three-body problem (CRTBP) by a continuation scheme described in Paper I. This scheme ensures that, for $e_j \neq 0$, all the trajectories of each family have the same initial conditions, in an inertial frame of reference, as the corresponding CRTBP ($e_j = 0$) trajectory from which they are continued (and, consequently, the same initial values of the osculating elements e and α). Hence a trajectory in this paper is defined by the initial conditions of the CRTBP trajectory from which it is continued (x_0, y_0, p_{x0}, c_0 , denoting, respectively, the initial co-ordinates in the x - and y -axis, the initial momentum along the direction of the x -axis and the Jacobi

Table 1. Summary of the initial conditions and main results for the families of trajectories IU, IIU, and IIIU discussed in the paper. The letter U denotes that the trajectories start at the unstable configuration. M and N stand for main and nearby trajectories. The tabulated values give the time, in units of 10^4 dimensionless units ($\sim 2 \cdot 10^4$ yr), at which the osculating eccentricity exceeded $e_{\text{crit}}^{\text{II}}$ or unity. The symbol \approx indicates that the eccentricity came very close to $e_{\text{crit}}^{\text{II}}$ but did not exceed it. In all cases $c_0 = -1.575$

Trajectories			$T_{\text{cJ}} = 13.23 T_J$		$T_{\text{cJ}} = 113.23 T_J$		$T_{\text{cJ}} = 1013.23 T_J$	
			$e > 0.58$	$e > 1$	$e > 0.58$	$e > 1$	$e > 0.58$	$e > 1$
IU $x_0 = -0.7350$ $\alpha_0 = 3.324 \text{ AU}$ $(0.638 \alpha_J)$ $e_0 = 0.150$	a	M			1	> 10	> 10	> 10
		N			4	> 10	> 10	> 10
	b	M			> 10	> 10	> 10	> 10
		N			> 10	> 10	> 10	> 10
	c	M			> 10	> 10	> 10	> 10
		N			> 10	> 10	9	> 10
	d	M			8	> 10	> 10	> 10
		N			6.5	> 10	> 10	> 10
IIU $x_0 = -0.7375$ $\alpha_0 = 3.318 \text{ AU}$ $(0.6377 \alpha_J)$ $e_0 = 0.156$	a	M			3	> 10	> 10	> 10
		N			5	> 10	> 10	> 10
	b	M	> 2	> 2	4	> 10	> 10	> 10
		N	2	2	6	> 10	> 10	> 10
	c	M			> 10	> 10	> 10	> 10
		N			> 10	> 10	≈ 10	> 10
	d	M			> 10	> 10	> 10	> 10
		N			> 10	> 10	> 10	> 10
IIIU $x_0 = -0.7400$ $\alpha_0 = 3.312 \text{ AU}$ $(0.6365 \alpha_J)$ $e_0 = 0.163$	a	M	> 10	> 10	≈ 6	> 10	> 10	> 10
		N	5.5	7.5	> 10	> 10	> 10	> 10

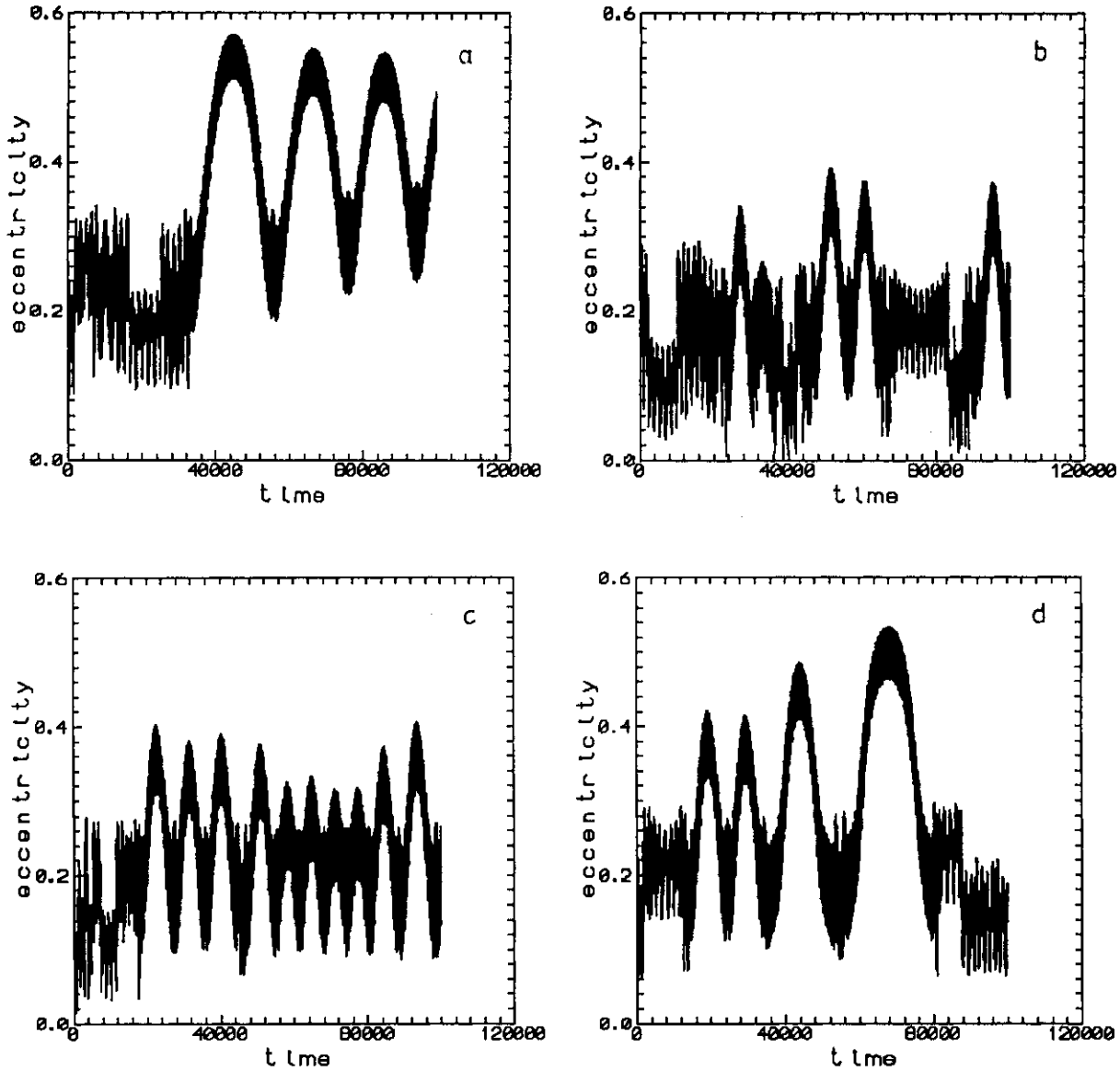
Table 2. Summary of the initial conditions and main results of the trajectories IVS and VS discussed in the paper. The letter S denotes that they are started at the stable configuration. The meaning of the symbols a–d, M and N as well as that of the tabulated values is discussed in the text and in Table 1. In all cases $c_0 = -1.575$

Trajectories			$T_{eJ} = 13.23 T_J$		$T_{eJ} = 113.23 T_J$	
			$e > 0.58$	$e > 1$	$e > 0.58$	$e > 1$
IVS $x_0 = -0.54$ $\alpha_0 = 3.308 \text{ AU}$ ($0.6357 \alpha_J$) $e_0 = 0.151$	a	M	75	75	251	>256
		N	30	40	>256	>256
	b	M	25	40	>660	>660
		N	>100	>100	290	>660
	c	M	30	30	>830	>830
		N	24	24	>830	>830
	d	M	75	75	451	495
		N	60	70	490	495
VS $x_0 = -0.53$ $\alpha_0 = 3.294 \text{ AU}$ ($0.6331 \alpha_J$) $e_0 = 0.163$	a	M	95	95		
		N	>100	>100		
	b	M	92	>100		
		N	>100	>100		
	c	M	75	75		
		N	>100	>100		
	d	M	>100	>100		
		N	26	26		

constant of the corresponding CRTBP trajectory) as well as by e_{Jmin} , e_{Jmax} and T_{eJ} . All the calculated trajectories here have $y_0 = p_{x0} = 0$, so that all trajectories start either at their apocenter or their pericenter. The first case corresponds to the “unstable” configuration and the second to the “stable” one (by analogy to the CRTBP, where these trajectories correspond to the stable and unstable periodic orbits). Note that, since our system is non-autonomous, one more initial condition is needed, namely the initial position of Jupiter on its orbit, given by its initial mean anomaly, u_0 . For each set of the above initial conditions we have calculated four, in all, trajectories of our model, denoted by the letters a–d, taking successively four values of u_0 corresponding to $t_0 = 0, \pi/2, \pi$ and $3\pi/2$ and, consequently, to $(\omega - \omega_J) = \pi, 3\pi/2, 0$ and $\pi/2$. To ensure that the observed behaviour of each trajectory reflects actual properties of the model and not spurious numerical instabilities, due to possible integration errors, we calculated, for any “main” trajectory (denoted by M in Tables 1 and 2), a second “nearby” trajectory (denoted by N in Tables 1 and 2), starting at a point $5 \cdot 10^{-6}$ dimensionless units away, in the x -direction, from the starting point of the main trajectory.

Before presenting our results, we should briefly discuss the problem of the integration accuracy, which was monitored by computing the value of the extended phase space Hamiltonian (which should be exactly zero). For all the calculated trajectories, the absolute value of this quantity, up to a time interval of $2 \cdot 10^5$ yr and before any close encounter with Jupiter, remained below 10^{-10} . All the trajectories were integrated in double precision using a Bulirsch–Stoer routine (Press et al. 1986). Some of them, including the near-escape trajectory presented in Fig. 4, were integrated, for confirmation purposes, twice, the second time in quadruple precision. It should be noted that small changes in the requested accuracy in the integration routine and/or in the precision used (double or quadruple) resulted, in some cases, in considerable deviations in the calculated evolution of e and α . These deviations, however, involved the *quantitative* behaviour *only* of the corresponding orbital element and not the qualitative one. In particular, as far as the appearance of the large-amplitude oscillations is concerned (connected to the evolution of e above e_{crit}^I , as described in what follows), only the time of onset, the period and (to a lesser extent) the amplitude of the oscillations were affected, and not their appearance in the first place, and this for integration intervals longer than 10^5 yr. Note that the values of e and α of the near-escape trajectory of Fig. 4 showed observable differences between the double- and quadruple-precision integrations only after the value of e approached unity.

Our results are presented in Tables 1 and 2 and Figs. 1–5. In the tables we give a summary of the initial conditions and results for five families of trajectories: three at the initial unstable configuration, denoted by U (Table 1), and two at the initial stable configuration, denoted by S (Table 2) for three values of the ratio T_{eJ}/T_J , i.e. 13.23, 113.23 and 1013.23 (other values were used as well with similar results). All trajectories have $c_0 = -1.575$ and e_{min} , e_{max} equal, respectively, to 0.03 and 0.06. The tabulated values, in the appropriate columns, give the time where the osculating eccentricity of the asteroid exceeded e_{crit}^I ($=0.58$) or 1, respectively. In Figs. 1–3 we show the typical evolution of the osculating eccentricity, e , of several continuation trajectories of trajectory IU (see Table 1 and Paper I). We observe that, in general, the behaviour of e follows two distinctive patterns: either it varies chaotically, taking values below e_{crit}^I , or it is locked in long period oscillations (showing sometimes a mean increase in amplitude), in which case its value may exceed e_{crit}^I or, even, e_{crit}^H (Figs. 1a, 1d, 2a, 2d, 3c). Notice, by the way, the similarity between the corresponding frames of Figs. 1 (main trajectories) and 2 (nearby trajectories), which indicates that the qualitative evolution of e is not due to any integration instabilities. The switching between these two patterns does not follow any obvious rule, although it seems that the locking into the long-period oscillation pattern is generic, in the sense that the numerical integration results indicate that it appears in all trajectories, provided they have been

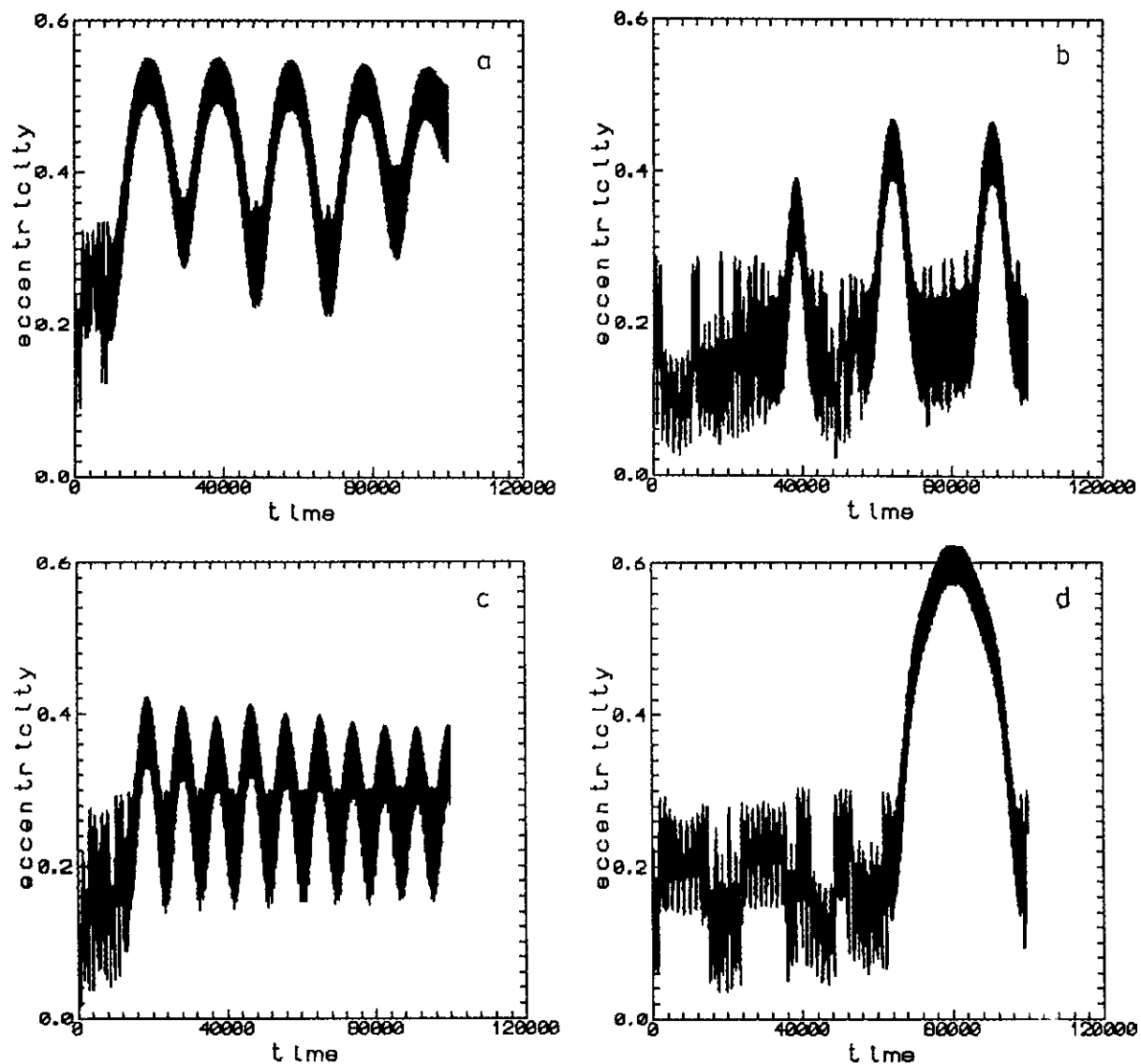


Figs. 1a–d. The evolution of the osculating eccentricity, e , of four continuation trajectories of trajectory IU ($c_0 = -1.575$, $x_0 = -0.7350$, $p_{x0} = y_0 = 0.0$, $\alpha_0 = 3.324$, $e_0 = 0.150$) for $e_{Jmin} = 0.03$, $e_{Jmax} = 0.06$ and $T_{eJ} = 113.23$ (main trajectories). **a** $t_0 = u_0 = 0$, $(\omega - \omega_J) = \pi$ **b** $t_0 = \pi/2$, $u_0 \approx \pi/2 + e_{J0} + O(e_{J0}^3)$, $(\omega - \omega_J) \approx 3\pi/2$, **c** $t_0 = u_0 = \pi$, $(\omega - \omega_J) = 0$ and **d** $t_0 = 3\pi/2$, $u_0 \approx 3\pi/2 - e_{J0} + O(e_{J0}^3)$, $(\omega - \omega_J) \approx \pi/2$

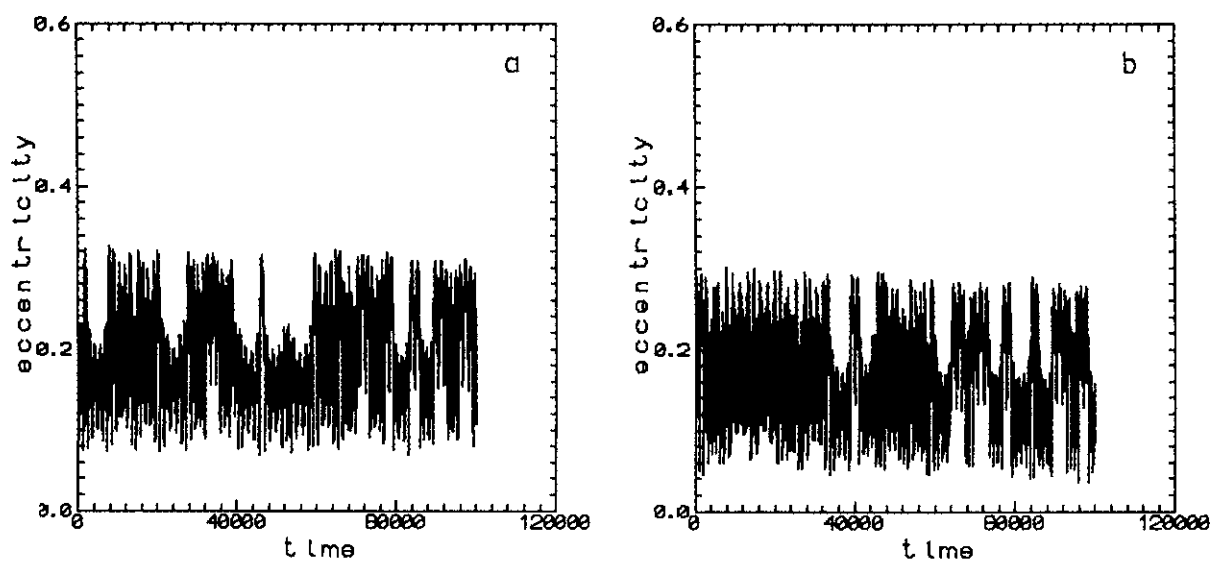
followed for a sufficiently long time interval. Furthermore, the amplitude and the period of these oscillations do not seem to depend on the specific value of T_{eJ} used, from $T_{eJ} \approx 10T_J$ up to $T_{eJ} \approx 1000T_J$ (note that the last value is of the same order of magnitude as the actual T_{eJ}), indicating that this phenomenon persists for values of T_{eJ} of the same order of magnitude as the actual period of the variation of e_J . Therefore it seems reasonable to postulate that a fictitious asteroid following such a trajectory may eventually undergo a close encounter with Mars or Jupiter, after which it will be removed from the 2:1 resonance region and, possibly, even from the main asteroidal belt. The first removal mechanism is not included in our model. One

would expect, however, the manifestation of the second removal mechanism in some of the calculated trajectories, provided that they are followed for a sufficiently long time interval, and this is in fact what we have found.

In Fig. 4 we show the long time evolution of some characteristic quantities of trajectory IIUbN for $T_{eJ} = 13.23T_J$. This trajectory was selected for a long-time integration because in Fig. 3 of Paper I its eccentricity shows, up to $t = 10^4$, a steady increase. In Fig. 4a we see that e tends, initially, to follow a long period oscillation with a period of $\sim 10^5$ and a maximum value of ~ 0.6 , which is interrupted by a close encounter with Jupiter. After this encounter the eccentricity (Fig. 4a) and the semi-major axis



Figs. 2a-d. Same as Fig. 1 but nearby trajectories ($x_0 = -0.7350 + 5 \cdot 10^{-6}$)



Figs. 3a-d. Same as Fig. 1 but $T_{ej} = 1013.23$ and nearby trajectories

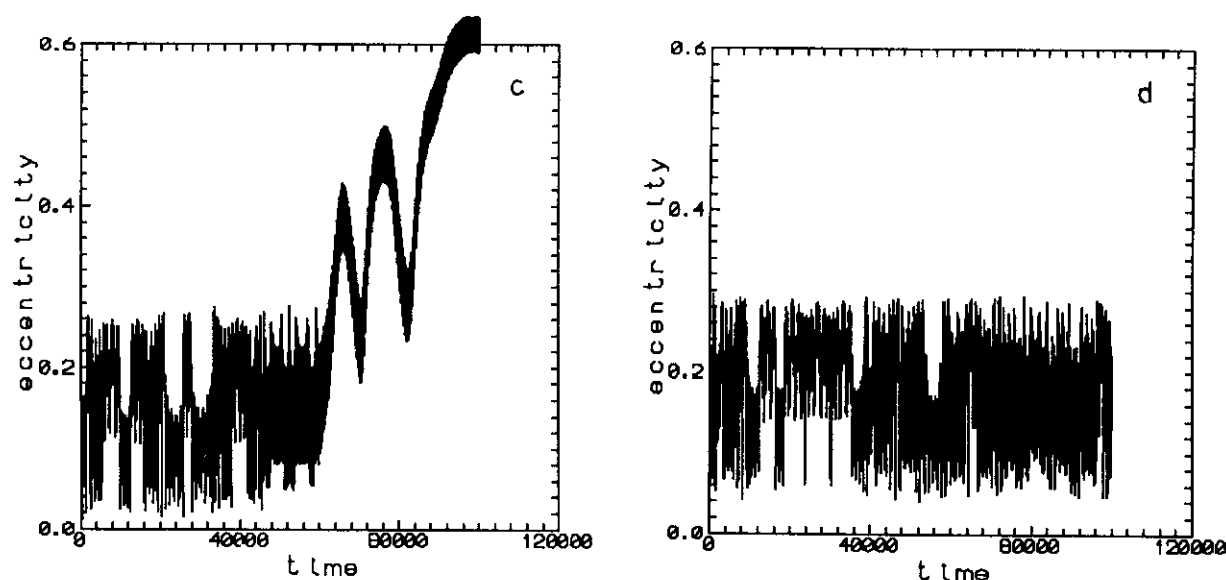


Fig. 3 (continued)

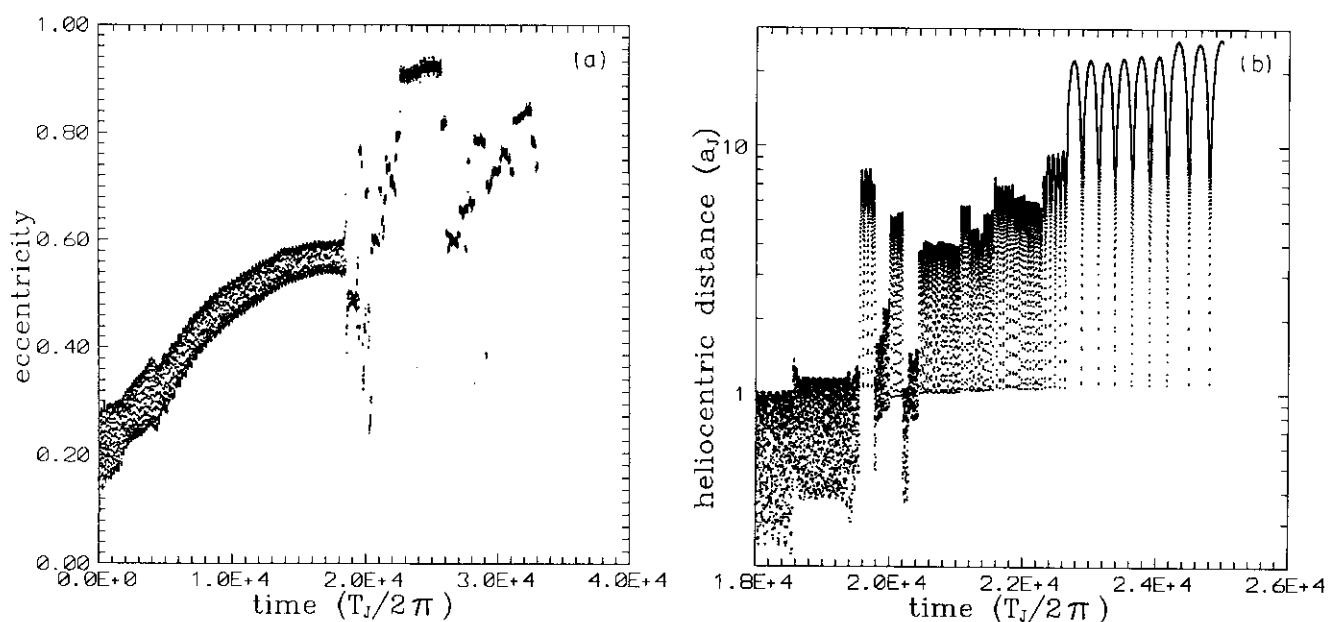


Fig. 4a. The evolution of the osculating eccentricity, e , of the nearby continuation of trajectory IIU with initial conditions $x_0 = -0.7375 + 5 \cdot 10^{-6}$, $c_0 = -1.575$, $y_0 = p_{x0} = 0$, $\alpha_0 = 3.318$ AU, $e_0 = 0.156$, $e_{jmin} = 0.03$, $e_{jmax} = 0.06$, $T_{ej} = 13.23 T_J$ and $t_0 = \pi/2$

Fig. 4b. The evolution of the heliocentric distance, r , of the trajectory of Fig. 4a. Notice that only the interval between $t = 1.8 \cdot 10^4$ and $2.6 \cdot 10^4$ is plotted, since the behaviour of r below the lower limit is trivial, while the one above the upper limit is uncertain

vary between $\sim .5 < e < \sim 1.0$ and $\sim 25 < \alpha < \sim 75$ AU respectively, while the heliocentric distance, r , (Fig. 4b) varies in the range $\sim 5 \text{ AU} < r < 150 \text{ AU}$.

Finally in Table 2 and Fig. 5 we show that the same qualitative behaviour seems to characterise the trajectories starting at the stable configuration, the only difference being that the eccentricity increase beyond the critical values appears after considerably longer (1–2 orders of

magnitude larger) time intervals. Due to this phenomenon we did not calculate any trajectory for $T_{ej}/T_J > 113.23$. It is worth to note that, although the time of appearance of the long period oscillations in the eccentricity of the trajectories, mentioned above, seems not to depend on the value of T_{ej} , the time of appearance of eccentricity values above e_{crit}^{II} or unit certainly depends, as it is obvious from Tables 1 and 2. This fact should be related to the specific process by

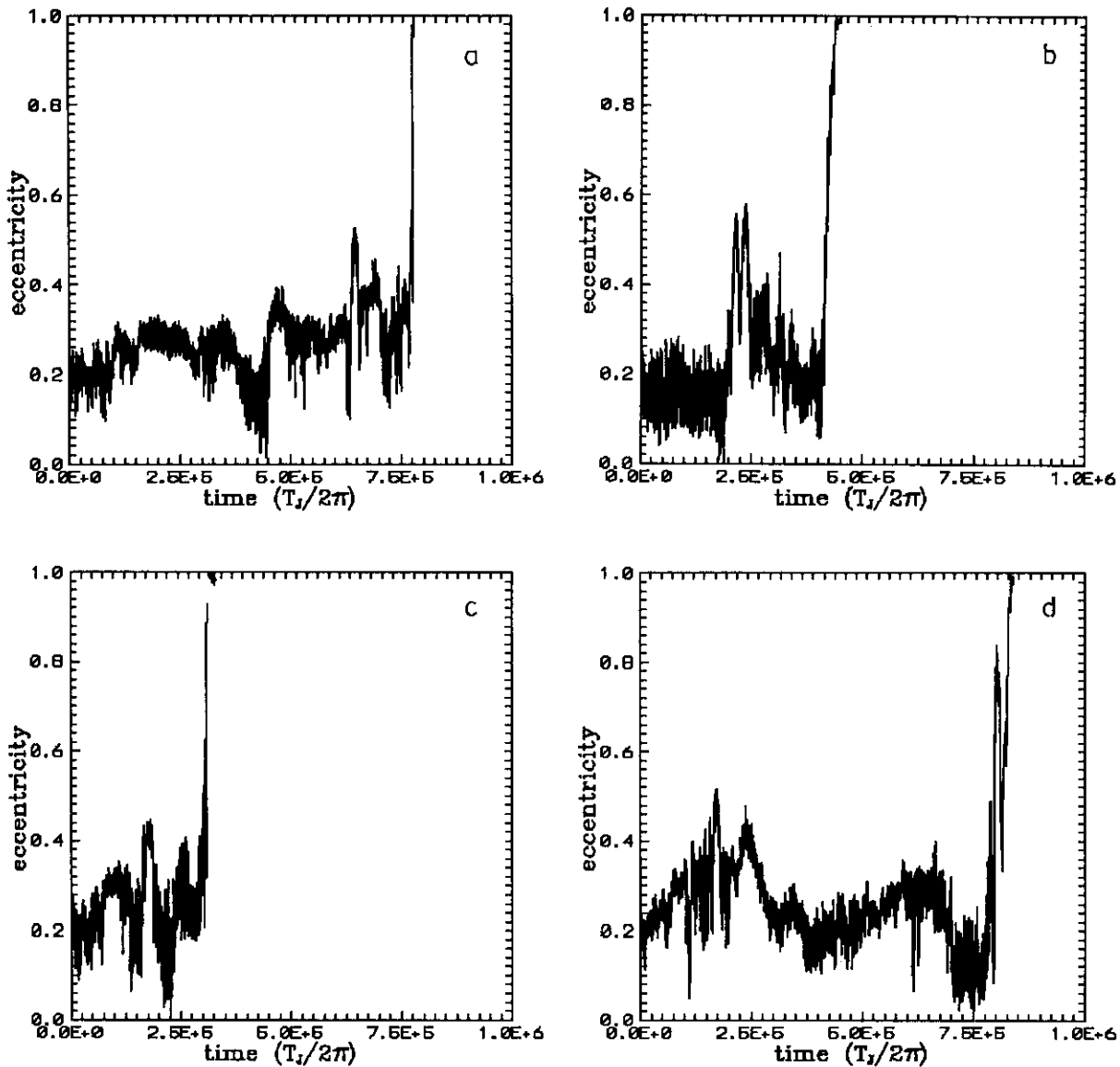


Fig. 5a–d. The evolution of the osculating eccentricity, e , of four continuation trajectories of trajectory IVS ($c_0 = -1.575$, $x_0 = -0.5300$, $p_{x0} = y_0 = 0.0$, $\alpha_0 = 3.308$, $e_0 = 0.151$) for $e_{\min} = 0.03$, $e_{\max} = 0.06$ and $T_{ej} = 113.23$ (main trajectories). For the difference between trajectories a–d see Fig. 1. Note that the integration was stopped when e exceeded unity, since this fact was followed by a severe loss of accuracy

which the trajectories migrate to phase space regions characterised by high eccentricities and it will be examined in a future work.

3. Conclusions

In conclusion we may say that the numerical evidence presented in this paper suggests that the dynamical model proposed by Varvoglis (1991) may give the qualitative behaviour of asteroid trajectories in the 2:1 resonance and, in particular, the expected increase of the osculating eccentricity for the actual value, T_{ej} , of the period of variation of e_j . Furthermore the model possesses solutions in which

an asteroid, starting either at the unstable (an already known result for the ERTBP, see Yoshikawa 1989, 1991) or the stable configuration, is removed from the distribution through a close encounter with Jupiter. Recent numerical integrations of the full three dimensional, four body problem (stable configuration) have shown exactly the same results, i.e. close encounters with Jupiter for time scales of the order of 10^7 yr, even for zero inclination values (Scholl & Froeschle 1993). Therefore the variation of Jupiter's eccentricity, alone, seems to be sufficient for the creation of the Kirkwood gap at the 2:1 resonance, so that our model may be used as a tool for a fast qualitative investigation of the evolution of the osculating eccentricity, e , of asteroid's

trajectories, in particular at the resonances where the ERTBP approximation fails to reveal any eccentricity increase beyond e_{crit}^I .

Acknowledgements. The author would like to thank Dr. M. Yoshikawa for a critical reading of the manuscript and for several useful comments.

References

- Hockney R.W., Eastwood J.W., 1981, Computer Simulation Using Particles, McGraw-Hill, New York, p. 335
Lemaitre A., Henrard J., 1990, Icarus 83, 391
Press W., Flannery B., Teukolsky S., Vetterling M., 1986, Numerical Recipes, Cambridge University Press, Cambridge
Scholl H., Froeschlé C., 1993 (private communication)
Varvoglis H., 1991, Earth, Moon and Planets 54, 257
Wisdom J., 1982, AJ 87, 577
Wisdom J., 1983, Icarus 56, 51
Wisdom J., 1987, Icarus 72, 241
Yoshikawa M., 1989, A&A 213, 436
Yoshikawa M., 1991, Icarus 92, 94